SUPPLEMENTAL MATERIALS AND METHODS

Antihistamines in Animal Models

Acute irritant contact dermatitis (AICD) model: Opposite ears of C57BL/J mice were treated topically with 20 μl of the phorbol ester, 12-O-tetradecanoylphorbol-13-acetate (TPA) (0.03%), and propylene glycol:ethanol (7:3 vols) to the opposite ear. Two hrs later, ear thickness was measured with calipers, and inflammation was assessed in H+E sections (Sheu*, et al.*, 2002, Fowler*, et al.*, 2003).

Female hairless mice (SKH1) were first sensitized with 2% oxazolone (Ox) applied topically to both ears. One week later, 0.05% Ox was applied either once, resulting in acute allergic contact dermatitis (AACD) model, challenged 3x or 10x, every other day, producing a subacute allergic contact dermatitis (SACD), or atopic dermatitis (AD)-like models, respectively (Man*, et al.*, 2008). At the end of the last challenge, mice were treated topically once with either 5% diphenhydramine, 5% cimetidine, 5% 2-pyridylethylamine dihydrochloride (H1 agonist), 5% dimaprit (H2 agonist), or vehicle alone, following which changes in basal TEWL, SC hydration and surface pH were assessed, and biopsy samples obtained, as above.

Histology, Histochemistry and Immunohistochemistry

Nile Red Staining: 5 μm frozen sections from biopsies of both antihistamine- and vehicle-treated animals were incubated with 0.0001% nile red in glycerin/water (75/25, v/v) (Man*, et al.*, 2006), and examined in a Zeiss microscope (Jena, Germany), with digital images captured with AxioVision software (Carl Zeiss Vision, Munich, Germany).

Histology and Immunohistochemistry: Changes in epidermal thickness were measured in random, transverse H+E-stained sections (n=10) from 3 different skin samples from each group,

and expressed as mean +/- SEM. Immunohistochemical assessment of both differentiation markers and proliferation were carried out as described (Komuves*, et al.*, 2000, Komuves*, et al.*, 2002). Briefly, after deparaffinization and blockade with 4% bovine serum albumin, 5μm sections were incubated overnight at 4°C with primary rabbit anti-mouse antibodies at dilutions of 1:2,000 for filaggrin, 1:1,000 for involucrin, and 1:500 for loricrin. After washing with 10mM citrate buffer, sections were incubated with goat anti-rabbit antibody (1:400) for 30 min at room temperature, followed by ABC-peroxidase reaction. For PCNA staining, sections were incubated with biotinylated monoclonal anti-PCNA antibody for 2 hrs at room temperature. Sections were visualized and images captured, as above.

Measurements of mRNA expression

mRNA expression was measured by real time quantitative PCR [rt(Q)-PCR] (suppl. Table 2) (Uchida*, et al.*, 2007). Briefly, total RNA was isolated from mouse epidermal sheets using STAT 60 (TEL TEST Inc. Friendswood, TX) and/or RNeasy 96 kit (Qiagen, Valencia, CA or Hilden, Germany). cDNA was prepared using reverse transcription, and mRNA expression was measured by rt(Q)-PCR using the iScript cDNA Synthesis kit (Bio-Rad Labs, Hercules, CA). For semi-qualitative PCR, we used the SYBR Green Master Mix (Applied Biosystems (ABI), Foster City CA) on an ABI machine. To confirm the appropriateness of amplification and size of PCR products, they were visualized on agarose gels (suppl. Fig. 1), and amplicons then were purified using QIAquick PCR purification kit (Qiagen), and sent for sequencing (Microsynth, Blagach, Switzerland). For all PCR studies, expression of mRNAs was normalized to GAPDH mRNA (levels did change after H1/2r antagonist applications).

Epidermal Lipid Synthesis

After four days of twice-daily topical applications of H1/2r antagonists, two hrs after tape stripping of normal skin, epidermal sheets were prepared by incubating full-thickness skin samples for 2 hrs at 37^0C in 2 ml of 10mM EDTA in calcium- and magnesium-free PBS, containing 40 μCi [^{14}C] acetate (Man*, et al.*, 1993, Man*, et al.*, 2006). After stopping further incorporation on ice, [^{14}C] acetate incorporation into epidermal fatty acids, cholesterol and total non-saponifiable lipids was determined by saponification, extraction, thin-layer chromatography, and quantitation of corresponding bands by scintillation counting (Feingold et al., 1990; Man et al. 2006).

Electron Microscopy

Biopsies from vehicle- and antagonist-treated mice (as above) were fixed in Karnovsky's fixative overnight, and post-fixed with either 0.25% ruthenium tetroxide or 1% aqueous osmium tetroxide (Hou*, et al.*, 1991). Ultrathin sections were examined in an electron microscope (Zeiss 10A, Carl Zeiss, Thornwood, NY) operated at 60 kV. Cornified envelope (CE) cross-sectional dimensions were measured in 60 micrographs from two separate vehicle, H1r, and H2r-treated samples. To optimize accuracy, only perpendicular sections were measured. Lamellar body density and secretion were assessed visually in randomly photographed, coded micrographs, without knowledge of the experimental group.

References:

Fowler, A J, Sheu, M Y, Schmuth, M, et al. (2003) Liver X receptor activators display anti-inflammatory activity in irritant and allergic contact dermatitis models: liver-X-receptor-specific inhibition of inflammation and primary cytokine production. *J Invest Dermatol* 120:246-55

Hou, S Y, Mitra, A K, White, S H, et al. (1991) Membrane structures in normal and essential fatty acid-deficient stratum corneum: characterization by ruthenium tetroxide staining and x-ray diffraction. *J Invest Dermatol* 96:215-23

Komuves, L G, Hanley, K, Lefebvre, A M, et al. (2000) Stimulation of PPARalpha promotes epidermal keratinocyte differentiation in vivo. *J Invest Dermatol* 115:353-60.

Komuves, L G, Schmuth, M, Fowler, A J, et al. (2002) Oxysterol stimulation of epidermal differentiation is mediated by liver X receptor-beta in murine epidermis. *J Invest Dermatol* 118:25-34

Man, M Q, Choi, E H, Schmuth, M, et al. (2006) Basis for improved permeability barrier homeostasis induced by PPAR and LXR activators: liposensors stimulate lipid synthesis, lamellar body secretion, and post-secretory lipid processing. *J Invest Dermatol* 126:386-92

Man, M Q, Feingold, K R and Elias, P M. (1993) Exogenous lipids influence permeability barrier recovery in acetone-treated murine skin. *Arch Dermatol* 129:728-38

Man, M Q, Hatano, Y, Lee, S H, et al. (2008) Characterization of a hapten-induced, murine model with multiple features of atopic dermatitis: structural, immunologic, and biochemical changes following single versus multiple oxazolone challenges. *J Invest Dermatol* 128:79-86

Sheu, M Y, Fowler, A J, Kao, J, et al. (2002) Topical peroxisome proliferator activated receptor-alpha activators reduce inflammation in irritant and allergic contact dermatitis models. *J Invest Dermatol* 118:94-101

Uchida, Y, Hama, H, Alderson, N L, et al. (2007) Fatty acid 2-hydroxylase, encoded by FA2H, accounts for differentiation-associated increase in 2-OH ceramides during keratinocyte differentiation. *J Biol Chem* 282:13211-9

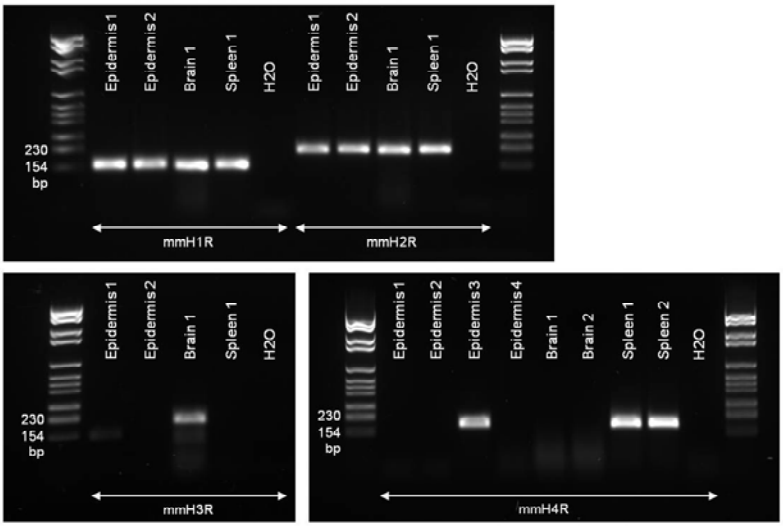

Suppl. Fig. 1: <u>H1r and H2r Are the Only Hr Expressed in Normal Mouse Epidermis</u>. cDNA was isolated from epidermal sheets obtained from C57B2/6 mice, as in Methods. Expected PCR products were: mmH1r – 153 bp, mmH2r – 218 bp, mmH3r – 213 pb, mmH4r – 181 bp (see suppl. Table 2), and the cDNA extracts were sequenced and gave the expected sequence. The gels show representative experiments.

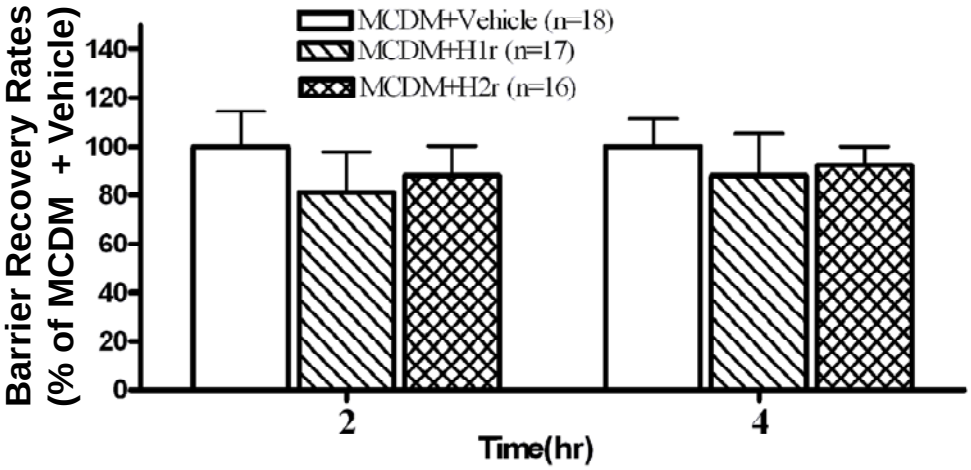

Suppl. Fig. 2: MCDM mice were treated with either the H1r or H2r antagonist or vehicle alone. Changes in barrier recovery kinetics of the H1/2r antagonists vs. vehicle-treated (100%) are shown. Neither achieved statistical significance.

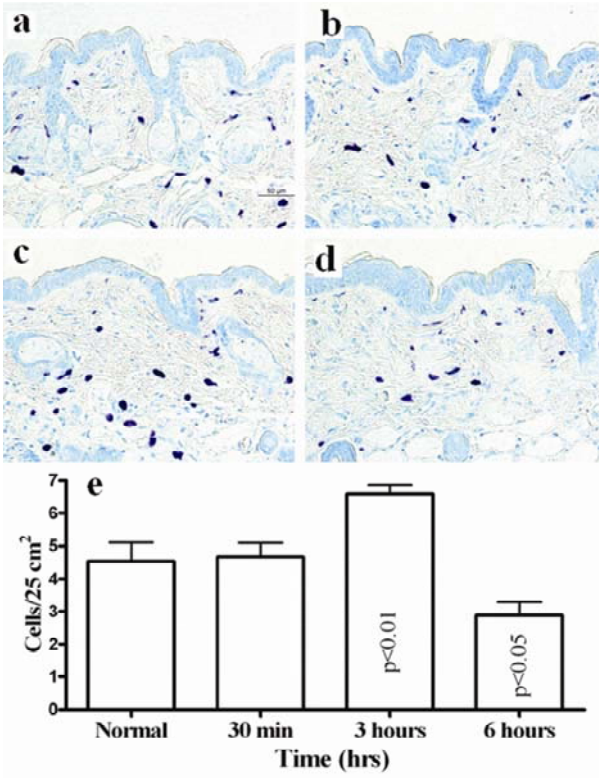

Suppl Fig. 3: a. normal skin; **b**. 30 min after barrier disruption; **c.** 3 hours after barrier disruption; **d.** 6 hours after barrier disruption, and **e.** quantitation of mast cell density after barrier disruption (n=17 for both normal and 3 hours after barrier disruption, n=18 for 30 min after barrier disruption, n=15 for 6 hours after barrier disruption). P values are compared with normal. Scale bar = 50 μm.

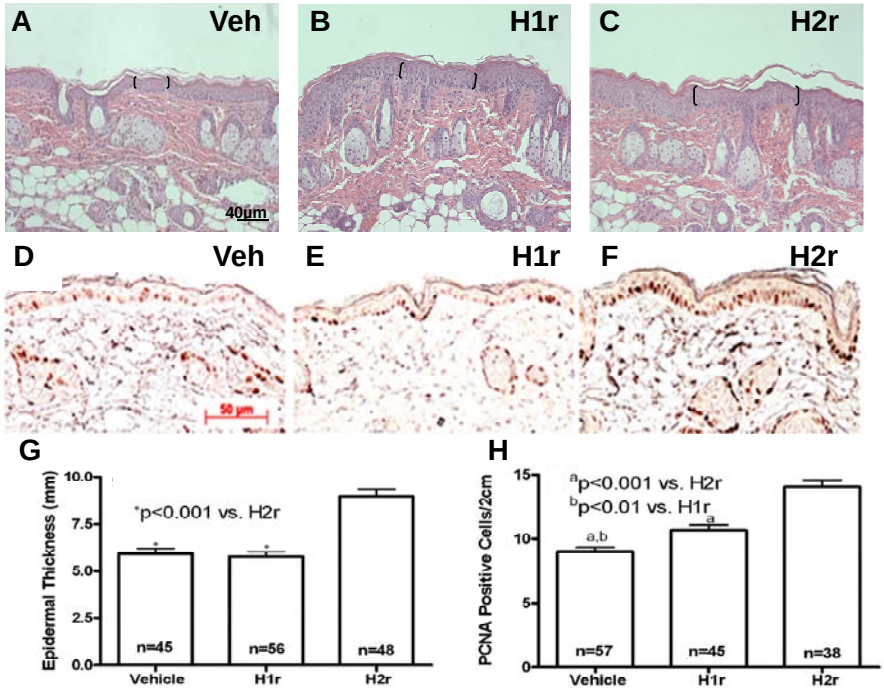

Suppl. Fig. 4: Topical Antihistamines Stimulate Epidermal Proliferation. The H1r/H2r antagonists or vehicle were applied, and biopsies were taken for H+E staining and PCNA immunostaining (Ki-67 nuclear protein antigen) after four days of treatment, as above (**A-F**). **G-H:** Quantitative data for changes in epidermal thickness and epidermal proliferation were quantitated (PCNA+ basal cells/μm length of basal layer) in randomized, coded micrographs from multiple sites and three separate biopsies.

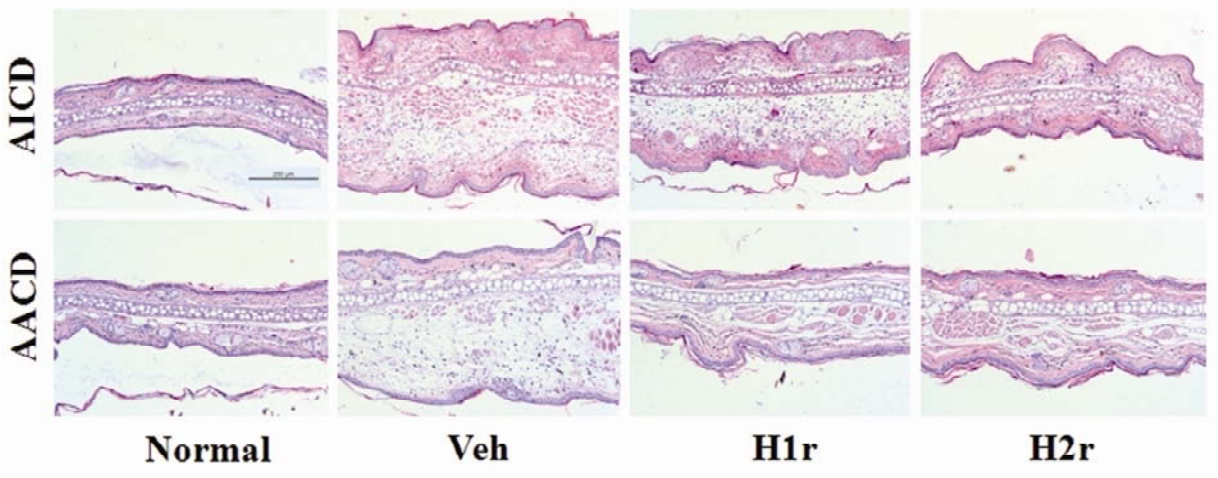

Suppl. Fig. 5: Histologic Evidence of Reduced Inflammation Following H1/2r Antagonist Applications to AICD (upper panel) and AACD (lower panel). AICD: acute irritant contact dermatitis; AACD: acute allergic contact dermatitis.

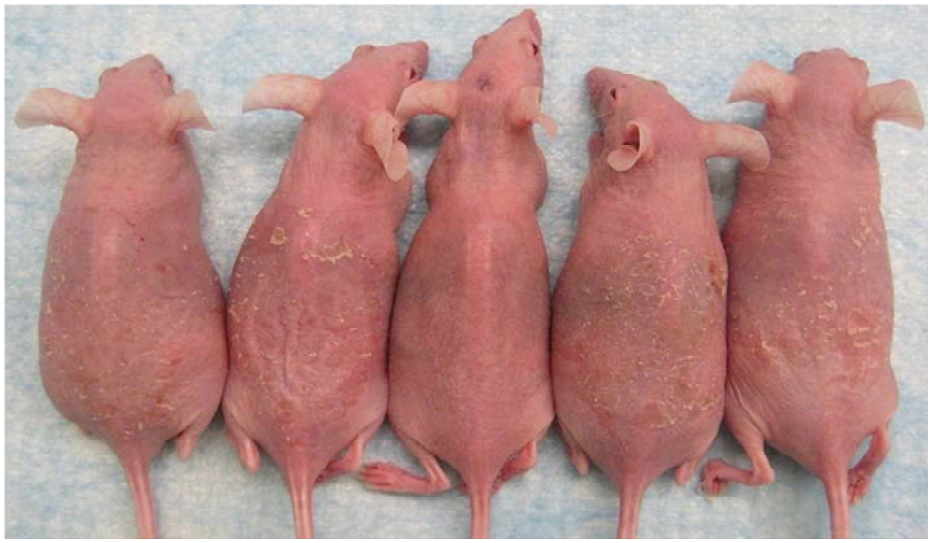

(10x)Ox + Veh +H1 agonist +H1 antagonist +H2 agonist +H2 antagonist

Suppl. Fig. 6: Topical H1r and H2r Antagonists Improve, while H1/2r Agonists Aggravate Inflammation/Scaling in Mouse Atopic Dermatitis Model. Animals shown are from a representative experiment (see Results and legend to Fig. 6).

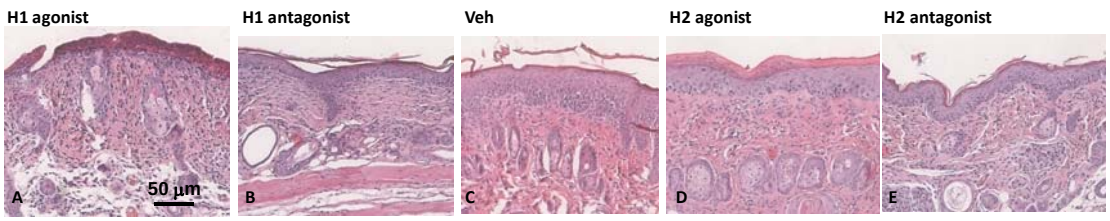

Suppl. Fig. 7: <u>Topical H1r and H2r Antagonists Improve, while H1/2r Agonists Worsen Epidermal Hyperplasia and Inflammation in Murine Atopic Dermatitis-Like Model</u>. A: Mice with established atopic dermatitis (AD)-like dermatosis were treated once with either the H1/2r antagonists (**B&E**), agonists (**A&D**) or vehicle alone (Veh) (**C**). Epidermal hyperplasia and inflammation is apparent in Veh-treated AD mice (**C**), and the inflammatory infiltrate further impinges on epidermis, inducing necrosis in H1/2r agonist-treated mice. Decreased epidermal hyperplasia, with less inflammation is apparent in H1r and H2r antagonist-treated mice. H+E sections (6 μM). Scale bar = 5 μm (all figures at same magnification).

Supplemental Table 1: Primers used for qRT and Semi-Qualitative PCR analyses

Gene	Forward Primer (5'–3')	Reverse Primer (5'–3')	Purpose
GAPDH	ACCTGCCAAGTATGATGACATCA	GGTCCTCAGTGTAGCCCAAGAT	qRT-PCR
Filaggrin	ATGTCCGCTCTCCTGGAAAG	TGGATTCTTCAAGACTGCCTGTA	qRT-PCR
HMGCoA R	CTTGTGGAATGCCTTGTGAT	CCGAAGCAGCACATGATC	qRT-PCR
Loricrin	GTGGAAAGACCTCTGGTGGA	TGGAACCACCTCCATAGGAA	qRT-PCR
Involucrin	AAGGGCTTTCCCAAACATGA	TGCTGGTGCTCACACTTTTGA	qRT-PCR
ACC	GGACAGACTGATCGCAGAGAAAG	TGGAGAGCCCCACACACA	qRT-PCR
FAS	GCTGCGGAAACTTCAGGAAAT	AGAGACGTGTCACTCCTGGACTT	qRT-PCR
K1	GGAAGGAGAGGAGATCAGGATGT	TGGTGTGGCTGGTGCTCA	qRT-PCR
ABCA12	AGGATGGCTTCCCAGTTTCA	TGGCCATAAGATCAAGACAAGTGT	qRT-PCR
SPT	ACTCGTCAGGAAATTGGAAACC	GGTCATAGCAGCTTCCACACCTA	qRT-PCR
FA2H	CGCTGGCTGGAGCAGTACTAT	TGCAGAGGCTACAGCACCATT	qRT-PCR
ELOVL4	CGATAAGCATAAGCACGCTCTATC	AACGGCTCGCGGTCTTTC	qRT-PCR
H1r	GACCTTGGTGGATCGACAGT	TGTCGGAATGTGAGCGAAG	semi-qualitative-PCR
H2r	GAAGACCTGCTGAGGCTGG	GCCCTGTGGCTTCTACACTC	semi-qualitative PCR
H3r	AGCTGTGGCTGGTGGTAGAC	CGGACAGGTACTCCCAACTC	semi-qualitative-PCR
H4r	TAGGCAATGCTGTGGTCATC	AGCCAAAACATGCAGATTCC	semi-qualitative-PCR

Supplemental Table 2: Characteristics of Inflammatory Dermatosis Models

Model	How Elicited	Barrier Function	Pathogenesis and Immunophenotype
Acute irritant contact dermatitis (AICD)	Topical phorbol ester (TPA)	Normal (see Results)	Epidermal-initiated cytokine cascade → non-specific inflammation
Acute allergic contact dermatitis (AACD)	Hapten (oxazolone) sensitization → single (Ox) challenge	Normal (see Results)	Antigen absorption stimulates th1-dominant inflammation
Subacute allergic contact dermatitis (SACD)	Ox sensitization → 3x Ox challenges	Abnormal (see Fig. 6)	Like AACD, with early features of AD, such as ↑serum IgE and th1→th2 mixed infiltrate
Atopic dermatitis (AD)-like dermatitis	Ox sensitization → 10x Ox challenges	Abnormal (see Fig. 6)	Barrier-induced cytokine cascade + ↑IgE; ↑mast cells and eosinophils; pure th2 infiltrate; reduced mBD3 and mCAMP